

# Robust DNN Watermarking via Fixed Embedding Weights with Optimized Distribution

Benedetta Tondi, *Member, IEEE*, Andrea Costanzo, Mauro Barni, *Fellow, IEEE*.

**Abstract**—Watermarking has been proposed as a way to protect the Intellectual Property Rights (IPR) of Deep Neural Networks (DNNs) and track their use. Several methods have been proposed that embed the watermark into the trainable parameters of the network (white box watermarking) or into the input-output mapping implemented by the network in correspondence to specific inputs (black box watermarking). In both cases, achieving robustness against fine tuning, model compression and, even more, transfer learning, is one of the most difficult challenges researchers are trying to face with. In this paper, we propose a new white-box, multi-bit watermarking algorithm with strong robustness properties, including retraining for transfer learning. Robustness is achieved thanks to a new information coding strategy according to which the watermark message is spread across a number of fixed weights, whose position depends on a secret key. The weights hosting the watermark are set prior to training, and are left unchanged throughout the entire training procedure. The distribution of the weights carrying out the message is theoretically optimised to make sure that the watermarked weights are indistinguishable from the other weights, while at the same time keeping their amplitude as large as possible to improve robustness against retraining. We carried out several experiments demonstrating the capability of the proposed scheme to provide high payloads with practically no impact on the network accuracy, at the same time retaining excellent robustness against network modifications and re-use, including retraining for transfer learning.

**Index Terms**—IPR protection, Deep Learning security, DNN watermarking, White box watermarking, Robust DNN watermarking

## I. INTRODUCTION

Deep Neural Networks (DNN) are nowadays used and commercialized in almost all fields due to the astonishing performance they achieve. Machine learning as a service (MLaaS) provided by large companies has also become a popular business paradigm. However, training a DNN model is a noticeable piece of work, that requires significant computational resources (the training process may go on for weeks, even on powerful machines equipped with several GPUs) and the availability of huge training data. Thus a trained DNN model can be treated as an Intellectual Property (IP) of the model owner. For this reason, the demand for methods to protect the IP Rights (IPR) associated to DNNs and trace the use and re-use of DNN models is rising. Watermarking has recently been proposed as a way to address these issues, and researchers have proposed several watermarking methods to protect the IPR of DNN models [1], [2].

Although DNN watermarking inherits some basic concepts and methods from classical media watermarking [3], [4], [5], embedding a watermark into a DNN and recovering it from the

watermarked model is a different piece of work with respect to media watermarking, calling for the development of new techniques tailored for this application scenario [6].

Robustness against network modifications and re-use is doubtless one of the most difficult challenges researchers have to face with in the field of DNN watermarking [2]. While there are some methods that can achieve remarkable robustness against model pruning and weight quantization, the great majority of the watermarking algorithms proposed so far, most noticeably multi-bit methods, offers very limited robustness against retraining. In addition, to the best of our knowledge, no method has been proposed so far achieving robustness against transfer learning, in the more general setting wherein the target task of the retrained network is different than that of the original network, a scenario often referred to as *inductive transfer learning* [7]<sup>1</sup>. In this scenario, the watermarked model is used as a pre-trained starting point to facilitate the learning of a different - yet related - task. This represents an important and very typical kind of network re-use, threatening the IPR of the DNN models, hence, devising a watermarking system achieving a satisfactory robustness in this scenario is of primary importance.

In this paper, we propose a white-box, multi-bit, watermarking algorithm achieving superior robustness against network modifications, including robustness against retraining in the most challenging inductive transfer learning scenario. As other schemes proposed so far (e.g., [8], [9], [10]), we adopt a Spread Spectrum (SS) approach [5], whereby the watermark is spread across several DNN coefficients. However, in our method, the values of the DNN weights hosting the watermark are controlled directly by the watermarking module prior to training, making sure that their amplitude is large enough to survive retraining and other modifications. The watermarked weights are then frozen and are not updated anymore during the learning phase. This marks a significant difference with respect to prior works, wherein the watermark is embedded implicitly during training, by adding a watermarking term to the training loss function [8], [9], [11], [12], thus losing the possibility to control directly the location and the amplitude of the watermarked coefficients, to improve the robustness of the watermark.

For a correct implementation of the above strategy, we must make sure that: i) the presence of the frozen watermarked weights does not impede achieving a high accuracy on the task the network is intended to solve; in fact, for high payloads and large spreading factors, when the number of watermarked weights is large, this is not an obvious result;

<sup>1</sup>The case where the source and target tasks are the same, and only the domain (hence the dataset) changes is referred to as *transductive transfer learning* scenario.

ii) the watermarked weights should not be easily identified, to avoid that the watermark is removed by possible attackers (watermark security) [13]. With regard to the latter point, the distribution of the pseudo-random spreading sequence and the watermarked coefficients, is optimised by minimizing the Kullback-Leibler (KL) divergence between the watermarked and non-watermarked weights for a given strength of the watermark.

The effectiveness of the proposed DNN watermarking algorithm is validated by considering different architectures and classification tasks for different application domains, namely, image classification and image manipulation detection. The results we got show that the proposed method can achieve good performance yielding high payloads with no impact on the accuracy of the baseline classification task. We also verified the strong robustness of the watermark against the most common network modifications, including, pruning, weights quantization, and, most noticeably retraining.

The main contributions of the paper can be summarized as follows:

- We propose a multi-bit static DNN watermarking algorithm based on spread spectrum, where the weights hosting the watermark are controlled directly by the watermarking module and then frozen during the learning phase. The values assigned to the watermarked weights are such that their amplitude is large enough to survive later modifications, e.g., during retraining.
- The distribution of the pseudo-random spreading sequence, determining the values of the watermarked weights, is theoretically optimised by minimizing the KL distance between the distribution of the watermarked and non-watermarked weights (for a given watermark strength).
- We run experiments considering different architectures and classification tasks. The experiments show that the proposed scheme can achieve high embedding payloads without impairing the performance of the network on the primary classification task, at the same time achieving strong robustness against all the most common network modifications, including retraining for transfer learning.

The rest of this paper is organized as follows: in Section II we provide a brief overview of prior art in DNN watermarking, and highlight the novelty of the proposed method with respect to previous works. In Section III, we introduce the notation used throughout the paper and state the requirements to be satisfied by the watermark. In Section IV we describe the watermark embedding and extraction algorithms. Section V and VI are devoted, respectively, to the description of the experimental setting and to the discussion of the experimental results. Finally, in Section VII, we draw our conclusions and highlight directions for future work.

## II. BACKGROUND ON DNN WATERMARKING AND PRIOR ART

DNN watermarking schemes exploit the high redundancy of deep neural networks and the consequent degrees of freedom in the choice of the model weights, to enforce learning the watermark information in addition to the desired task. The

requirements that any DNN watermarking scheme must satisfy follow the so-called watermarking trade-off triangle [6], originally introduced for media watermarking, depicting the necessity of finding a good tradeoff among three conflicting requirements, namely, *capacity*, *unobtrusiveness* and *robustness*. Capacity, more correctly indicated as payload, has exactly the same meaning as in media watermarking: it measures the number of information bits conveyed by the watermark. Unobtrusiveness refers to the capability of the watermarked network to accomplish the task it is thought for. Finally, robustness is related to the possibility of correctly extracting the watermark from a modified version of the model, e.g. after retraining or model pruning.

Robustness against network re-use is a very challenging requirement that can be achieved only up to a very limited extent by the schemes developed so far [2], [14], [15], [16], [17].

A detailed taxonomy of DNN watermarking techniques has been introduced in [2]. A first distinction regards multi-bit and zero-bit watermarking. As in traditional media watermarking, in the multi-bit case, the message bits are embedded inside the network and the watermark detector has to extract them without knowing them in advance. For zero-bit watermarking, instead, the detector must only decide about the existence of a specific, known, watermark. In DNN watermarking, distinction is also made between *static* and *dynamic* watermarking. Static DNN watermarking methods embed the watermark directly into the internal trainable parameters of the network, typically the weights of the DNN model. Both embedding and extraction require white-box access to the internal parameters of the watermarked models. Some examples of static methods can be found in [8], [18], [9], [11], [19], [20]. In dynamic watermarking schemes, instead, the watermark is associated to the behaviour of the network in correspondence to specific inputs, called trigger or key inputs, see for instance [21], [22], [23], [24], [16]. Even in this case, the watermark is eventually stored in the network weights, however it is retrieved indirectly by looking at the effect that the presence of the watermark has on the behaviour of the network. Typically, the watermark is recovered by looking at the output of the model, when the model is queried with a set of properly chosen inputs. In this way, the watermark is extracted in a black-box way, only requiring API access to the model. There are also some works that associate the watermark to the activation maps of some (internal) neurons, e.g., [25], [26], in which case white-box extraction is required.

In this paper, we focus on multi-bit, static, watermarking. The seminal work for this kind of methods, is the one introduced by Uchida et al. in [8]. Embedding is achieved by adding a proper regularization term to the loss function during training, in such a way to enforce a correct extraction of the embedded bits. Later on, several methods have been proposed to improve the performance of Uchida's algorithm. In [18], Uchida's algorithm is used to implement a traitor tracing watermarking system with anti-collusion capabilities. An improvement of [8] has been proposed in [27], where the use of Adam optimization and a secret transformation matrix is proposed to increase the robustness against pruning for a similar detectability of the watermark. The authors introduce

a novel method based on orthogonal projections to solve the detectability problem that arises when watermarking a DNN which is being optimized with Adam. A side effect of this novel method is an increased robustness against weight pruning

Among other methods developed starting from [8] we mention the approaches in [11], [12], [10], [9]. In particular, in [9], a different loss function is considered for embedding, to extend the use of the informed coding paradigm to DNN watermarking. The method proposed in [9] can achieve a larger payload with lower impact on network accuracy (unobtrusiveness) compared to [8], while retaining a similar level of robustness.

A drawback with all the DNN watermarking methods developed so far (both static and dynamic) is that the watermark is not very robust against network re-use and in particular model retraining. By focusing on zero-bit watermarking, a static scheme with improved robustness against retraining has been proposed in [15]. The algorithm adopts a properly designed loss function explicitly thought to increase the robustness of the watermark by making the watermarked weights more sensitive to loss variations with respect to normal weights. Therefore, when retraining is performed starting from the watermarked model, changes to the weights bearing the watermark will be penalized. The method in [15] can achieve remarkable robustness against fine-tuning, when the network is further trained additional epochs on the same data,<sup>2</sup> and weights quantization, however robustness against transfer learning is still missing.

In this work, we overcome the drawback of lack of robustness of DNN watermarking methods (especially, multi-bit ones) and propose a static, multi-bit DNN watermarking algorithm that is robust against transfer learning. In particular, robustness is achieved in the more general inductive transfer learning scenario, when the model is re-trained on a different task and different domain. Our method has some similarity with the scheme proposed in [15], since even in [15], the weights hosting the watermark are fixed before training and are not modified during the training process. The strategy adopted in our scheme to enforce robustness against network manipulation, however, is completely different, since we achieve it by augmenting the amplitude of the weights hosting the watermark, while at the same time making sure that they are statistically indistinguishable from the other weights. As we will show later, in this way we are able to achieve a remarkable robustness against a wide range of network manipulations, including transfer learning, which was out of reach of [15], despite the adoption of a more favourable zero-bit watermarking setting.

### III. NOTATION, WATERMARKING MODEL AND REQUIREMENTS

#### A. Preliminaries

To start with, we introduce the main notation and concepts used in the rest of the paper.

<sup>2</sup>In fine-tuning, the model is re-trained on the same task and domain (same dataset or a subset of it), eventually with a different learning rate.

We let  $\Phi$  generically indicate a non-protected model, that is, a model trained for a given task without the watermark. Notation  $\Phi^m$  is used to denote the watermarked model. We denote with  $\mathcal{L}$  the loss function of the network, that usually corresponds to the cross-entropy function. The average loss measured across all the samples of the labeled training set  $(\mathcal{X}, \mathcal{Y})$  is compactly denoted with  $\mathcal{L}(\mathcal{X}, \mathcal{Y}, \Phi)$  (or  $\mathcal{L}(\mathcal{X}, \mathcal{Y}, \Phi^m)$ , for the watermarked model).

We indicate with  $\mathbf{b} \in \{0, 1\}^l$  the vector with the watermark bits, (sometimes referred to as the watermark message), where  $l$  denotes the number of bits the watermark consists of, that is, the the payload.

Network weights can be generically represented as tensors. For each convolutional layer  $j$ , the dimensionality of the weight parameter tensor for that layer is determined by the kernel size of the filters, the depth of the input and the number of filters (3-dim tensor). For notational simplicity, we flatten the weight tensor into a vector  $\mathbf{w}_j$  (row vector) containing all the weights of layer  $j$ . We generically indicate the vector with all the weights of the network (be it watermarked or not) as  $\mathbf{w}$ . With the above notation, embedding the watermark bits into the weights of the network corresponds to embed the vector  $\mathbf{b}$  into the vector  $\mathbf{w}$ . The final watermarked vector should be such that the network preserves its functionality. Given that unobtrusiveness can not be controlled directly by modifying the weights of the model, typically, in DNN watermarking embedding is carried out during training, contextually to the learning procedure used to make sure that the network solves the task is intended for.

We denote with  $\Omega$ , hereafter called *host* index set, the set with the indexes of the network weights hosting the watermark, that is, the positions in  $\mathbf{w}$  that are selected to carry out the watermark message<sup>3</sup>. The cardinality of  $\Omega$  is indicated by  $n$  ( $n \geq l$ ). With this notation, the vector with the watermarked weights should be indicated as  $\mathbf{w}^m = (w_{i_1}, w_{i_2}, \dots, w_{i_n}), i_k \in \Omega$ , however, for sake of simplicity, we will indicate it as  $\mathbf{w}^m = (w_1^m, w_2^m, \dots, w_n^m)$ . We also introduce the vector with non-watermarked coefficients, indicated by  $\bar{\mathbf{w}}^m$ . With the notation introduced above, we have  $\bar{\mathbf{w}}^m = (w_{j_1}, w_{j_2}, \dots, w_{j_n}), j_k \notin \Omega$ , more simply written as  $\bar{\mathbf{w}}^m = (\bar{w}_1^m, \bar{w}_2^m, \dots, \bar{w}_{N-n}^m)$ , where  $N$  is the total number of coefficients the model consists of. We observe that the host indexes may be selected from only one layer (single-layer embedding), or multiple layers (multi-layer embedding). We find useful to denote with  $\Omega_k$  the set of watermark indexes in layer  $k$ . By indicating with  $N_k$  the number of weights in layer  $k$ , then, the percentage of watermarked weights in the network, denoted with  $p^m$ , is equal to  $p^m = |\Omega|/N \times 100$ , while the percentage of watermarked weights in layer  $k$  is  $p_k^m = |\Omega_k|/N_k \times 100$ . We let  $f_{\mathbf{w}^m}$  and  $f_{\bar{\mathbf{w}}^m}$  denote the marginal empirical distribution of the watermarked and non-watermarked weights, estimated over  $\mathbf{w}^m$  and  $\bar{\mathbf{w}}^m$  respectively, that is, the distributions induced by

<sup>3</sup>For simplicity, we refer to the weights specified by the host indexes as host weights; however, the concept of host signal does not have the same meaning it has in media watermarking, given that in DNN watermarking the weights do not exist *per se* but are directly generated in such a way to host the watermark.

the respective sequences, and let  $E_{w^m}$  (res.  $E_{\bar{w}^m}$ ) denote the empirical expectation computed over  $f_{w^m}$  (res.  $f_{\bar{w}^m}$ ). Finally, we denote with  $\mathcal{D}$  the Kullback-Leibler (KL) distance between two continuous probability distributions  $f$  and  $g$  [28], defined as  $\mathcal{D}(f||g) = \int_{x \in \mathbb{R}} f(x) \log(f(x)/g(x)) dx$ .<sup>4</sup>

### B. Watermarking model and requirements

In the setting adopted in this paper, the model owner wants to embed a watermark message  $\mathbf{b}$  into the weights  $\mathbf{w}$  of the watermarked model  $\Phi^m$ . To do so, he relies on a secret key  $K$ , providing the information on the host layers and weights, that is  $\Omega$ . The secret key also includes the spreading sequence used to spread the message  $\mathbf{b}$  over the watermark coefficients. Watermark extraction requires white-box access to the network, hence qualifying our scheme as a white-box watermarking algorithm [2].

The watermark must satisfy the following properties.

- **unobtrusiveness**: the presence of the watermark should not affect the capability of the watermarked network to accomplish the task it is thought for, that is, the accuracy of  $\Phi^m$  should be similar to that of  $\Phi$ .
- **integrity**: in the absence of model modifications, the extracted watermark  $\hat{\mathbf{b}}$  should be close (ideally equal) to  $\mathbf{b}$ , that is, in the absence of modifications the bit error rate should be small (ideally zero).
- **robustness**: it should be possible to recover the message  $\mathbf{b}$  also from a modified version of the network.
- **payload**: the payload of the watermark, that is the length of the message  $\mathbf{b}$ , should be large as large as possible.

Regarding the robustness requirement, we consider several kinds of model re-use and modifications, that are routinely carried out by network users: retraining for fine tuning and in particular transfer learning, and model compression, namely, parameter pruning and weights quantization.

- **Retraining**: retraining represents a typical modification that network models undergo. The network model is further trained for some epochs on the same or a different task. We speak about *fine-tuning* when the network model is retrained for the same task and on the same domain (often, on the same dataset used for the original training or on a subset of it), for some additional epochs, possibly with a different learning rate. We speak about *transfer learning* in a more general retraining framework where the knowledge is transferred across domains or tasks. While, in fact, some knowledge is specific of individual domains and tasks, there is some knowledge which is common across different domains and tasks. Transfer learning is widely adopted in practice since it turns out that transferring the knowledge is by far less computationally expensive with respect to training the model from scratch. By referring to the categorization adopted in [7], in the *transductive transfer learning* setting, the source and target tasks are the same, while the source and target domains are different (when many labeled

data from the source domain are available, while few labeled data from the target domain are available, the model can be first trained on the source domain and then trained some additional epochs on data belonging to the target domain). In the *inductive transfer learning* setting, the target task is different from the source task, while the domain can be the same or not. In this case, the model trained on the source task is used as a pre-trained solution to train a network on a new task, possibly related to the original one (e.g., when a network pre-trained on ImageNet is used to train a model for traffic sign classification or food classification). Retraining alters the weights of the model, the degree of alteration depending on the difference in the domain and task considered for the retraining, with respect to those considered for the original training, and on the number of retraining epochs. Arguably, during transfer learning, the weights are modified by a much larger extent than during fine-tuning, thus achieving robustness in the former scenario can be much harder.

- **Compression**:

DNN models are often squeezed to deploy them into low power or computationally weak devices, and to reduce the storage demand so that models can be loaded in storage-limited devices, like mobile devices. Typical methods for model compression are *network pruning* and *weight quantization*. The former cuts off network weights, whose activation value is smaller than a threshold, the latter reduces the numerical precision of the model parameters, converting floating point (typically, models are trained in floating-point 32-bit arithmetic) to a lower-precision representation, typically integer point representations. More specifically, the quantization procedure can be summarized as follows:

$$\mathbf{w}_q = \left\lfloor \frac{\mathbf{w}}{\delta} \right\rfloor \times \delta, \quad \delta = 2w_{max}/2^{n_b}, \quad (1)$$

where  $\mathbf{w}_q$  indicates the quantized weights,  $w_{max}$  represents the maximum absolute value assumed by the weights, and  $n_b$  indicates the number of bits required to represent the quantized values.

We observe that network retraining represents the most critical case of network re-use for existing DNN watermarking schemes. Although some DNN watermarking methods have been proposed that can achieve remarkable robustness against fine-tuning [15], in fact, to the best of our knowledge, no method can achieve robustness in a transfer learning scenario.

## IV. THE PROPOSED DNN WATERMARKING METHOD

In this section we describe the watermark embedding (Section IV-A) and extraction (Section IV-B) procedures.

### A. Robust watermarking algorithm

The main intuition we exploit to embed a watermark that can survive retraining even in a transfer learning scenario is that the network weights change slowly during the iterations, so if we embed the watermark into - many - large coefficients

<sup>4</sup>For discrete distributions the integral is replaced with a summation over the input alphabet of  $x$ .

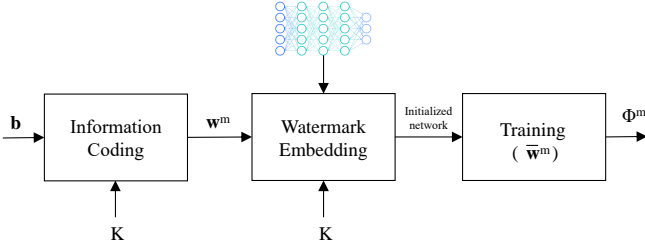


Fig. 1: Watermark embedding procedure.

and the number of retraining epochs is limited the watermark will survive retraining. Despite its simplicity, this idea comes with two major challenges. To start with, we must make sure that the presence of several fixed large coefficients does not prevent the possibility of training an efficient network. Secondly, we must avoid that the large coefficients hosting the watermark are easily identified and attacked. For this reason we optimize the distribution of the marked coefficients to make them as indistinguishable as possible from the non marked ones.

Specifically, the proposed watermark embedding algorithm works according to the following principles:

- The information message  $\mathbf{b}$  is embedded before training and the weights hosting the watermark message, i.e., the watermarked weights, are not updated during training.
- The message bits are encoded in  $\mathbf{w}^m$  via direct sequence spread spectrum watermarking [5]. As a consequence, the message  $\mathbf{b}$  is spread over several host weights thus increasing its robustness. Specifically, the  $l$  bits of the message are used to modulate a pseudo-random sequence of length  $n$  ( $\gg l$ ), where  $S = n/l$  is the spreading factor. The strength of the watermark is controlled by means of a parameter  $\gamma$ .
- To make sure that the watermarked weights are indistinguishable from the other weights<sup>5</sup>, the distribution of the spreading sequence is chosen in such a way to be as close as possible to that of the non-watermarked weights. In particular, for a given  $\gamma$ , the optimum distribution of the sequence coefficients is derived theoretically by minimizing the KL divergence between the distribution of the watermarked and non-watermarked coefficients.

For a given payload of  $l$  bits, the trade-off between unobtrusiveness and robustness is determined by the spreading factor  $S$  and the strength  $\gamma$ . In particular,  $\gamma$  also controls the detectability of the watermark, with a too large  $\gamma$  resulting in an easy-to-detect watermark.

The main steps of the watermark embedding algorithm are summarized in Fig. 1. The details of each block are discussed in the following, where we first detail the encoding and the embedding process (Section IV-A1), then we describe the optimization we solved to determine the distribution of the pseudo-random spreading sequence used for the embedding (Section IV-A2).

<sup>5</sup>In this way we prevent that the watermarked weights can be easily detected and then dropped to remove the watermark from the network.

1) *Watermark embedding*: Let  $\mathbf{u} \in \{-1, +1\}^l$  be the antipodal sequence associated to  $\mathbf{b}$ , that is  $u_i = 1$  (res.  $-1$ ) if  $b_i = 1$  (res.  $0$ ). Before embedding, the vector  $\mathbf{u}$  is used to modulate a longer spread-spectrum sequence. In particular, each  $u_i$  is used to modulate a block of coefficients of a pseudo-random sequence of length  $n$  (direct sequence spread spectrum [5]).

Formally, given a spreading factor  $S$ , a pseudo-random sequence  $\mathbf{x} \in \mathbb{R}^n$  of length  $n = S \cdot l$  is generated (the generation of  $\mathbf{x}$  is discussed in Section IV-A2). Then, for each  $i \in [1, l]$ ,  $u_i$  is used to modulate the sign of the elements of  $\mathbf{x}$  corresponding to the indexes from  $S(i-1) + 1$  to  $Si$ . Specifically, the vector of watermarked coefficients  $\mathbf{w}^m$ , is obtained as follows:

$$w_j^m = u_i \cdot x_j, \quad j \in \{S(i-1) + 1, \dots, Si\}, \quad i \in [1, l]. \quad (2)$$

Then,  $(w_{S(i-1)+1}^m, \dots, w_{Si}^m)$  is the vector of the weights associated to the message element  $b_i$ . In the embedding phase, the network weights in the positions indicated by  $\Omega$  are initialized to the values given by  $\mathbf{w}^m$ .

With regard to the coefficients hosting the watermark, they are chosen at random according to a secret key  $K$ . It is worth observing that the secret key  $K$  rules both the selection of the host indexes in  $\Omega$  and the generation of the pseudo-random sequence  $\mathbf{x}$ . Given the watermarked network, both the host indexes and the pseudo-random sequence are required in order to read the watermark. In addition to security, a further advantage of choosing the positions of the watermarked weights randomly is that the weights associated to the same bits are more likely to undergo different (independent) changes during subsequent network modifications.

The network, then, is trained as follows: the network weights (and biases) are initialized randomly, thus getting the initial vector of the weights  $\mathbf{w}^{(0)}$ . The weights in the positions indicated by  $\Omega$ , are set to the values given by  $\mathbf{w}^m$ , that is, we set  $\{w_i^{(0)}\}_{i \in \Omega} = \mathbf{w}^m$ . At this point, the network is trained as usual, by minimizing the loss across all the samples of the labeled training samples  $(\mathcal{X}, \mathcal{Y})$ . The watermarked weights  $\mathbf{w}^m$  are frozen during the training process, and only the non-watermarked weights  $\bar{\mathbf{w}}^m$  (and, obviously, the biases) are updated through backpropagation.

As we said, a challenge of the proposed method is to make the watermarked weights as indistinguishable as possible from the non-watermarked weights, in order to avoid that they can be easily identified and then attacked. To this purpose, the distribution of  $\mathbf{x}$ , and then, as a consequence, the distribution of the watermarked weights  $\mathbf{w}^m$ , is chosen in such a way to minimize the distinguishability between watermarked and non-watermarked weights, as described in the following section.

2) *Optimization of the watermarked weights distribution*: We formalize below the problem of finding the optimum sampling distribution for generating the pseudo-random sequence used in (2) for the embedding.

Although our final goal is to optimize the distribution of the spreading sequence  $\mathbf{x}$ , hence, equivalently, from (2), of the watermarked weights  $\mathbf{w}^m$ , we find convenient to initially formulate the optimization problem as a minimization carried out over  $\mathbf{w}^m$ , given the direct dependence of the objective

function on the weights. Then, we will see that, under some mild assumptions, we can rephrase the optimization over the weights as an optimization over the weights distribution  $f_{\mathbf{w}^m}$ .

The problem of training a DNN watermarked model can be conveniently formalized as follows:<sup>6</sup>

$$\min_{\bar{\mathbf{w}}^m} \mathcal{L}(\mathcal{X}, \mathcal{Y}, \bar{\mathbf{w}}^m \cup \mathbf{w}^{m,*}) \quad (3)$$

where, in order to minimize the distinguishability between watermarked and non-watermarked weights,  $\mathbf{w}^{m,*}$  is obtained by solving the following optimization:

$$\mathbf{w}^{m,*} = \arg \min_{\mathbf{w}^m} \mathcal{D}(f_{\mathbf{w}^m} \| f_{\bar{\mathbf{w}}^m}), \quad (4)$$

which also depends on  $\bar{\mathbf{w}}^m$ , with the additional constrain that

$$E_{\mathbf{w}^m}[w|w > 0] = \gamma, \quad E_{\mathbf{w}^m}[w|w < 0] = -\gamma, \quad (5)$$

to control the average strength of the weights bearing the watermark.

We require that the watermarked weights distribution is symmetric (given that the distribution of the non-watermarked weights is typically symmetric, this goes w.l.o.g.). With this assumption, in fact, the watermarked weights  $w_j^m$  obtained via Eq. (2) follows the same distribution of the pseudo-random sequence  $\mathbf{x}$ , regardless of  $\mathbf{u}$ . Because of the symmetry of the distribution, we can rephrase the last equation as  $E_{\mathbf{w}^m}[|w|] = \gamma$ . A large  $\gamma$  results in a strong - hence expectedly more robust - watermark, possibly at the price of a bigger impact on the accuracy of the watermarked model. Moreover,  $\gamma$  affects the security. A very large value of  $\gamma$ , i.e., such that  $E_{\bar{\mathbf{w}}^m}[|w|] \ll \gamma$ , would, in fact, make the presence of the watermark easily detectable upon inspection of the values of the weights.

We observe that (3) and (4) are entangled equations due to the presence of  $\mathbf{w}^m$  and  $\bar{\mathbf{w}}^m$  in both of them, so they can not be solved easily. However, under the assumption that the presence of the watermark does not affect the statistical distribution of the non-watermarked weights<sup>7</sup>, the two minimizations can be separated as follows:

$$\mathbf{w}^{m,*} = \arg \min_{\mathbf{w}^m} \mathcal{D}(f_{\mathbf{w}^m} \| \tilde{f}_{\bar{\mathbf{w}}^m}) \quad (6)$$

$$E_{\mathbf{w}^m}[|w|] = \gamma,$$

$$\bar{\mathbf{w}}^{m,*} = \arg \min_{\bar{\mathbf{w}}^m} \mathcal{L}(\mathcal{X}, \mathcal{Y}, \bar{\mathbf{w}}^m \cup \mathbf{w}^{m,*}), \quad (7)$$

where  $\tilde{f}_{\bar{\mathbf{w}}^m}$  is the distribution of the non-watermarked weights of a non-watermarked model  $\Phi$  solving the same task.

To a closer look, we observe that the minimization in (6) depends only on the probability density function of  $\bar{\mathbf{w}}^m$  rather than on the specific sequence, so it can be conveniently reformulated as a minimization over the distribution  $f_{\mathbf{w}^m}$ :

$$f_{\mathbf{w}^m}^* = \arg \min_{f_{\mathbf{w}^m}} \mathcal{D}(f_{\mathbf{w}^m} \| \tilde{f}_{\bar{\mathbf{w}}^m}) \quad (8)$$

$$E[|w|] = \gamma,$$

<sup>6</sup>Rigorously speaking, the set of trainable parameters also includes the biases, that are not considered in the formulation since they are of no interest in the optimization, thus only complicating the notation.

<sup>7</sup>We checked experimentally that this assumption is satisfied, that is that the distributions of the weights corresponding to the non-host indexes in the non-watermarked model and that of watermarked model are approximately the same, for all the watermark setting considered in this paper. More details are reported in Section VI-A1.

yielding the optimum distribution  $f_{\mathbf{w}^m}^*$ . Then, the sequence  $\mathbf{w}^{m,*}$  appearing in (6) can be *any* sequence generated according to  $f_{\mathbf{w}^m}^*$ , thus allowing to keep the specific sequence  $\mathbf{w}^{m,*}$  secret and include it in the watermark key  $K$ .

Solving the problem in (8) for a general distribution of the non-watermarked weights  $\bar{\mathbf{w}}^m$  is not easy. In the following we solve it by assuming that the distribution of the non-watermarked weights can be approximated by a Laplacian distribution (our experiments on several network architectures and tasks confirmed this assumption, see Section VI-A1).

Let, then,  $\tilde{f}_{\bar{\mathbf{w}}^m}(w) = \frac{1}{2\lambda} e^{-|w|/\lambda}$ , that is  $\bar{w}_i^m \sim \text{Laplace}(0, \lambda)$ . Under such an assumption, problem (8) is solvable in close form, with the solution given by the following theorem.

**Theorem 1.** *Let  $\mathcal{F}$  denote the set of symmetric distributions. The minimization problem*

$$\min_{f_w \in \mathcal{F}} \mathcal{D}(f_w \| \frac{1}{2\lambda} e^{-|w|/\lambda}), \quad (9)$$

$$s.t. E[|w|] = \gamma$$

is equivalent to the problem of finding the maximum entropy distribution over all the symmetric probability density functions  $f_w$  satisfying  $E[|w|] = \gamma$ , whose solution is  $f_w^* = \frac{1}{2\gamma} e^{-|w|/\gamma}$ . Hence the optimum distribution for the watermarked weights is a Laplacian distribution with 0 mean and scale parameter  $\gamma$ , that is  $w_i \sim \text{Laplace}(0, \gamma)$ , for  $i \in \Omega$ .

*Proof.* By observing that

$$\mathcal{D}(f_w \| \frac{1}{2\lambda} e^{-|w|/\lambda}) =$$

$$\int_w f_w(w) \left[ \log f_w(w) - \log \frac{1}{2\lambda} e^{-|w|/\lambda} \right] dw =$$

$$\int_w f_w(w) \log f_w(w) dw - \log \frac{1}{2\lambda} - \frac{1}{\lambda} \log e \cdot E[|w|], \quad (10)$$

and given that  $E[|w|] = \gamma$ , (9) can be rephrased as

$$\max_{f_w} h(f_w) \quad (11)$$

$$E[|w|] = \gamma$$

where  $h(f) = -\int_x f(x) \log f(x) dx$  denotes the differential entropy. Equation (11) is equivalent to finding the *maximum entropy distribution* over all the probability density functions for which  $E[|w|] = \gamma$  [28].

By rewriting the differential entropy function integrating in the positive and negative support separately and exploiting the symmetry of  $f_w$  we get

$$h(f_w) = - \int_{\mathbb{R}} f_w(w) \log f_w(w) dw =$$

$$= -2 \int_0^{\infty} f_w(w) \log f_w(w) dw$$

$$= - \int_0^{\infty} f_w'(w) \log f_w'(w) dw + 1$$

$$= h(f_w') + 1, \quad (12)$$

where in the second-to-last equality we let:

$$f_w'(w) = \begin{cases} 2f_w(w) & w \geq 0 \\ 0 & w < 0 \end{cases}. \quad (13)$$

Therefore, in order to find the entropy-maximizing distribution in (11) we can equivalently solve the following problem

$$\begin{aligned} \max_{f'_w} \quad & h(f'_w) \\ E[w] = \quad & \gamma \\ f'_w(w) = \quad & 0, \text{ for } w < 0. \end{aligned} \quad (14)$$

The distribution we search for in (14) is the maximum entropy distribution over all the probability densities with support set  $[0, \infty)$  satisfying  $E[w] = \gamma$ . The solution of this problem is known ([28], Ex 12.2.5) and corresponds to  $f'_w = \frac{1}{\gamma} e^{-|w|/\gamma}$ ,  $w \geq 0$ , hence yielding:

$$f_w^*(w) = \frac{1}{2\gamma} e^{-|w|/\gamma}, -\infty \leq w \leq \infty. \quad (15)$$

□

Based on the result of Theorem 1, the watermarked weights have to be generated following the distribution  $f_{w^m}^* = \frac{1}{2\gamma} e^{|w|/\gamma}$ , that is,  $w^{m,*} \sim \text{Laplace}(0, \gamma)$ . To do so, we proceed as follows: we first generate the pseudo-random sequence  $\mathbf{x}$  according to a  $\text{Laplace}(0, \gamma)$  distribution. Then, we apply Eq. (2) to modulate the spreading sequence according to the watermark message, thus getting the vector of watermarked weights  $w^{m,*}$  following the same  $\text{Laplace}(0, \gamma)$ .

### B. Watermark extraction

Watermark retrieval requires the knowledge of the indexes of the watermarked weights and the pseudo-random sequence  $\mathbf{x}$  (both included in the secret key  $K$ ). The vector  $w^m$  is first obtained by reading the weights of  $\Phi^m$  in the positions indicated by  $\Omega$ , then the  $i$ -th bit of the watermark message is extracted as follows:

$$\hat{b}_i = \begin{cases} 1 & \text{if } \sum_{j=S(i-1)+1}^{S_i} x_j \cdot w_j^m \geq 0 \\ 0 & \text{otherwise.} \end{cases} \quad (16)$$

The Bit Error Rate (BER) is calculated as  $\text{BER} = \sum_i (\mathbf{b} \oplus \hat{\mathbf{b}})_i / l$ , where  $\oplus$  denotes the bitwise XOR operation.

We notice that, in the absence of modifications of the watermarked model,  $\hat{\mathbf{b}}$  is equal to  $\mathbf{b}$  by construction. In classical watermarking theory, such a property can be achieved only by informed watermarking algorithms [5], in which case embedding is performed by applying a signal-dependent perturbation to the host signal.

*In this case, the watermark can be recovered with no errors. In our paper, we exploit the completely different paradigm of DNN watermarking, pertaining watermarking of functionals instead of signals [6], to propose a method where the non-watermarked parameters, responsible for the desired functionality of the network, adapts to the watermark signal, hence being defined in a watermark-dependent way. Drawing a parallelism with the informed embedding paradigm and the theory of writing in a dirty paper by Costa [29], the dirt is represented by the watermark signal, injected in a white paper, instead of by the host signal like in classical watermarking*

## V. EXPERIMENTAL METHODOLOGY AND SETTING

We validated the proposed technique for DNN watermarking considering different architectures and classification tasks. Below, we describe the architectures, datasets and setting considered in our experiments.

### A. Host networks and tasks

We focused on tasks taken from two different application areas, that is, image forensics and pattern recognition. Specifically, we considered the following tasks: the forensic problem of detecting images generated by Generative Adversarial Networks (GANs) [30] (GAN image detection), the problem of traffic sign classification (GTSRB classification [31]), and object classification, namely CIFAR10 classification [32]. The selected tasks permit to test the effectiveness of our method in different scenarios, that is, the case of binary classification (GAN detection) and the case of multi-class classification with different number of classes (43 for GTSRB and 10 for CIFAR). For each task, we chose a network architecture among those achieving state-of-the-art performance. Specifically, for the GAN detection task, we considered the problem of discriminating natural and synthetic face images generated by the StyleGAN2 generative model [33], using XceptionNet, that can achieve state-of-the-art performance [34]. We trained the network for 10 epochs with Adam optimizer, learning rate 0.01 and batch size 32. More details on network training and the dataset can be found in the authors' repository ([35]). For the GTSRB and CIFAR10 tasks, we trained a DenseNet169 architecture [36]. Specifically, for GTSRB, the network was trained for 20 epochs with Adam optimizer, learning rate 0.001 and batch size 64, reaching the benchmark accuracy (<https://benchmark.ini.rub.de/>). For CIFAR10 classification, we trained the network following the parameter setting reported in [37], that yields state-of-the-art performance for the task. Notably, despite the similar number of parameters (around  $21 \times 10^6$  for DenseNet and  $13 \times 10^6$  for XceptionNet), XceptionNet and DenseNet are quite different architectures, both in terms of depth (with DenseNet having 603 layers in contrast to the 136 layers of XceptionNet), and internal structure connections. While the block connections in the XceptionNet architecture are pretty standard, in DenseNet, there are dense blocks where each convolutional layer is connected to every other layer in a feed-forward fashion.

Since the results of the experiments are similar for GTSRB and CIFAR10, for sake of brevity, we will provide an in-depth analysis for the GTSRB case, and a summary of the results for CIFAR10.

The DNN watermarking algorithm and network training have been implemented by using TensorFlow 2.5.0, via the Keras API. The code is publicly available for reproducibility at the address <https://github.com/andreacos/Deep-Neural-Networks-Robust-Watermark>.

### B. Watermarking algorithm setting

We tested the performance of our watermarking algorithm by considering both single-layer and multi-layer embedding.

Arguably, the multi-layer embedding solution is necessary for very large payloads and/or spreading factors, that is, for a very large  $n$ , when the percentage of watermarked weights in the watermarked layer for the single-layer embedding is too large, thus deteriorating the network performance, as confirmed by the experiments.

A summary of the layers considered in our experiments for watermark embedding for XceptionNet and DenseNet is reported in Table I. In all the cases, the host layers that we considered are convolutional network layers from intermediate to deep. The variance of the distribution of the non-watermarked weights is also reported for each layer ( $\sigma_k$ ), together with the total number of weights ( $N_k$ ). A noticeable difference between the two networks is that, the variance of the distribution of the weights in DenseNet is much lower than the variance of the weights in XceptionNet. This is the case regardless of the task accomplished by the network and is mainly a consequence of the different structure of the two networks. Therefore, a larger watermark strength can be considered in the XceptionNet case, with respect to the DenseNet case, for the same level of indistinguishability of the watermark.

In the multi-layer embedding case, for simplicity, we watermarked the same number of weights for each layer, that is  $|\Omega_k|$  is the same for all  $k$ 's. Given that the host layers have different number of parameters, i.e.  $N_k$  is different for every  $k$ , the percentage of the watermarked weights  $p_k^m$  are different. Such percentages are not reported in the table since they depend on the specific watermarking setting, i.e., on the payload  $l$  and on the spreading factor  $S$ . For a given host layer  $k$ , the watermark is embedded considering different strengths  $\gamma$  proportional to the variance  $\sigma_k$  of the distribution of the non-watermarked weights for the layer. In the experiments, we let  $\gamma = C\sigma_k$  and adjusted the watermark strength by varying the parameter  $C$ .

To watermark the GAN detection model based on XceptionNet, we considered  $C \in [0.7, 1.3]$ , while for the DenseNet models we considered integer values of  $C$  ranging from 2 to 20. These values are chosen based on an analysis of the indistinguishability of the embedded watermark. More discussion is provided in Section VI-A1.

### C. Setting for retraining experiments

The setting of the experiments we carried out to assess the robustness against retraining is described below. For the transfer learning scenario, we considered the more general inductive transfer learning setting. The watermarked protected models are then re-trained on a different task and different domain. Specifically, we used the watermarked protected models as pre-trained solutions and performed the new training using the standard loss, i.e, the cross-entropy loss  $\mathcal{L}$  (then, the watermarked weights are updated as well). Different transfer learning scenarios have been considered, as detailed below.

- 1) *Different tasks with the same number of classes.* We retrained the model initially trained to solve the GAN detection task to solve a new two-class classification problem, namely the classification of image picturing

cats and horses. Retraining is performed on 20K images for each class, taken from the LSUN dataset [38].

- 2) *Different tasks with different number of classes.* We retrained the model initially trained on GTSRB data (43 output nodes) to solve the CIFAR10 (10 output nodes) classification problem, and viceversa.

In both cases, the networks are trained for 10 epochs that are sufficient to reach the state-of-the-art accuracy on the new task.

We also assessed the robustness against fine-tuning, i.e., retraining the watermarked models for further epochs (10) on a subset of the training data. Retraining for fine-tuning is performed on 70% of the data (due to the significant imbalance among classes, especially in the GTSRB case, some classes would be very poorly represented by using a lower percentage). For the GAN detection task, where a very large huge number of images is available for training, we also tried fine-tuning on 30% of the datasets obtaining similar results.

## VI. RESULTS AND DISCUSSION

In this section, we report and discuss the results of the experiments we carried out to demonstrate that our algorithm can achieve large payloads without impairing the performance of the host models (Section VI-A), while at the same time achieving outstanding robustness against network modifications and re-use (Section VI-B). In particular, we show that the watermark can survive transfer learning, a result that can not be achieved by the state-of-the-art methods proposed so far.

### A. Performance of DNN watermarked models

Here we evaluate the drop in classification accuracy due to the presence of the watermark. The performance of the watermarked models are assessed by measuring the Test Error Rate (TER) = 1 - ACC, where ACC is the accuracy of the network on the classification task, and the BER, pertaining watermark extraction.

The results of our experiments on the GAN detection task for various embedding payloads ( $l$ ), watermark strengths ( $C$ ) and spreading factors ( $S$ ), are reported in Table II. The total number of watermarked weights ( $|\Omega|$ ) is also reported.

The TER(%) of the baseline non-watermarked model is 0.55%. When  $l = 256$ , and  $S = 6$ , the difference in the TER of the watermarked models compared to the baseline model is a negligible one. Since the position of the host weights is known during the extraction, the integrity requirement is satisfied by construction, and the BER is always equal to 0 (hence it is not reported in the table). A good TER can still be obtained with the single-layer embedding when the payload is  $l = 1024$  bits and  $S = 6$ . When  $S$  increases to 10 with  $l = 1024$ , embedding all the bits in the 2 layers leads to a too large  $p^m$ , compromising the unobtrusiveness, and a 4 layer setting has to be considered for the embedding. In this case TER = 0.66%. The same behavior occurs when we try to embed  $l = 2048$  bits in 2 layers, with  $S = 6$ , in which case the percentage of watermarked weights in the first layer goes far above 50%. We found that, for  $l = 2048$  bits, we need to

<sup>8</sup>The two sets are referred to as Set#1 (first row) and Set#2 (second row).



TABLE I: Summary of host layers settings and related information.

Architecture	Single/ Multi-layer	Host layers	$\sigma_k$	$N_k$
XceptionNet	1 layer	block14_sepconv2	1.8098	13824
	2 layers	block14_sepconv1, block14_sepconv2	[1.1378, 1.8098]	[9216, 13824]
	4 layers	block13_sepconv1, block13_sepconv2, block14_sepconv1, block14_sepconv2	[2.3441, 0.4284, 1.1378, 1.8098]	[6552, 6552, 9216, 13824]
DenseNet	1 layer	conv5_block16_1	0.00069	143360
	2 layers	conv5_block16_1, conv5_block20_1	[0.00069, 0.00057]	[143360, 159744]
	4 layers <sup>s</sup>	conv4_block16_1, conv4_block20_1, conv5_block16_1, conv5_block20_1 conv5_block16_1, conv5_block20_1, conv5_block24_1, conv5_block28_1	[0.00056, 0.00062, 0.00069, 0.00057] [0.00069, 0.00057, 0.00073, 0.00064]	[94208, 110592, 143360, 159744] [143360, 159744, 176128, 192512]

TABLE II: Performance of DNN watermarked models for the GAN detection task. The baseline TER is 0.55 %.

$l$	$S$	$C$	Layers	$ \Omega $	$p_k^m$ (%)	TER(%)
256	6	0.7	1	1536	11.0	0.61
	6	1	1	1536	11.0	0.44
	6	1.3	1	1536	11.0	0.77
1024	6	1	1	6144	44.44	0.31
	6	1	2	6144	[33.34, 22.22]	0.30
	10	1	2	10240	[55.56, 37.04]	35.43
	10	1	4	10240	[39.70, 39.70, 27.77, 18.51]	0.66
2048	6	1	2	12288	[66.67, 44.44]	38.74

TABLE III: Performance of DNN watermarked models for the GTSRB task. The baseline TER is 6.12%.

$l$	$S$	$C$	Layers	$ \Omega $	$p_k^m$ (%)	TER(%)
256	6	2	1	1536	1.1	6.23
	6	10	1	1536	1.1	4.46
	6	15	1	1536	1.1	3.93
	12	2	2	3072	[1.1, 1.0]	5.44
	12	10	2	3072	[1.1, 1.0]	5.37
	12	15	2	3072	[1.1, 1.0]	5.76
	20	15	2	5120	[1.78, 1.60]	6.89
1024	20	15	2	20480	[10.9, 9.2]	5.79
	10	15	4	10240	[2.7, 2.3, 1.8, 1.6]	4.91
	15	15	4 (1)	15360	[4.1, 3.5, 2.7, 2.4]	5.56
	20	15	4 (1)	20480	[5.4, 4.6, 3.6, 3.2]	5.79
	25	15	4 (1)	25600	[6.8, 5.8, 4.5, 4.0]	6.12
	15	15	4(2)	15360	[2.7, 2.4, 2.2, 2.0]	5.33
	20	15	4(2)	20480	[3.6, 3.2, 2.9, 2.6]	4.30
2048	20	15	2	40960	[21.7, 18.5]	3.56
	25	15	2	51200	[27.2, 23.1]	4.23
	25	15	4(2)	51200	[8.9, 8.0, 7.3, 6.6]	5.77

embed the watermark in more than 4 layers to get a good TER. We observed that, in order to embed large payloads without affecting the unobtrusiveness, we have to consider multiple-layers, in such a way that the percentage  $p_k^m$  for each layer  $k$  remains below 40%.

Table III reports the results for GTSRB classification. The results are reported for both single and multi-layer embedding and different host convolutional layers. For the case of 4-layer embedding, the set number (Set#) is reported among brackets. The BER is not reported, being always equal to 0. In this case, the TER of the baseline non-watermarked model is 6.12% (Acc = 93.88%), which is similar to the TER achieved by the watermarked models. Notably, in some cases, the TER is even significantly lower for the watermarked models, in which case the watermark acts as a regularizer. Although all the models achieve good TER, not all of them offer good robustness against retraining (see the discussion in Section VI-B).

The investigation of the limits of the proposed watermarking

system in terms of capacity, that is the characterization of the size of the payload that can be achieved without impacting significantly the TER, is an interesting one, and is left as future work.

#### 1) Analysis of weights distribution (watermark security):

We analyzed the distributions of the networks weights for normal models and watermarked models to experimentally validate the assumption made in our theoretical analysis and the indistinguishability of the watermarked weights.

Fig. 2 shows the distribution of the non-watermarked weights in the non-watermarked model (left) and in the watermarked model (right) for the case of Xception-based GAN detection (first row) and DenseNet-based GTSRB classification (second row). The watermark setting for the GAN detector is  $l = 256$ ,  $S = 6$ ,  $C = 1$ , single-layer embedding, while for the GTSRB classifier the figure reports the case  $l = 1024$ ,  $S = 15$ ,  $C = 15$ , 4-layers (Set#1), where  $|\Omega| = 15360$ . The distributions are similar in the other settings. By looking at the distributions for the normal models, we observe that they approximate reasonably well a Laplacian distribution, thus justifying our assumption (the Laplacian fitting is reported in the plots). Moreover, as argued, the presence of the watermark does not affect much the overall distribution, the shape being similar for both the normal and watermarked models. This is especially the case with the DenseNet model.

Fig. 3 shows the distribution of the weights in the embedding layer, both of the watermarked (red) and non-watermarked (blue) weights. From top left to bottom right, the same GAN watermarked model and GTSRB watermarked model are considered in the first and second plot, while the third plot shows the distributions for a GTSRB watermarked model corresponding to a different setting for the watermark, with a much larger number of watermarked weights, that is  $l = 2048$ ,  $S = 25$ ,  $C = 15$ , 2-layers, where  $|\Omega| = 51200$  (in contrast to  $|\Omega| = 15360$  of the other setting). The name of the embedded layer is reported in the plots.

For the GAN watermarked model, the plot shows the distribution of the weights for the single watermarked layer 'block14\_sepconv2'. Since the variance of the distributions of the watermarked and non-watermarked weights is similar with  $C = 1$  (the former being  $\sigma_k = 1.79$  and the latter  $\sigma_k = 1.81$  for the setting in the figure)<sup>9</sup>, no visible tails are introduced,

<sup>9</sup>We remind that we make the variance of the watermarked weights proportional (with constant  $C$ ) to the variance of the weights for the normal (non-watermarked) model of the same layer. In the watermarked model, the variance of the non-watermarked weights may be not exactly the same as in the normal model.

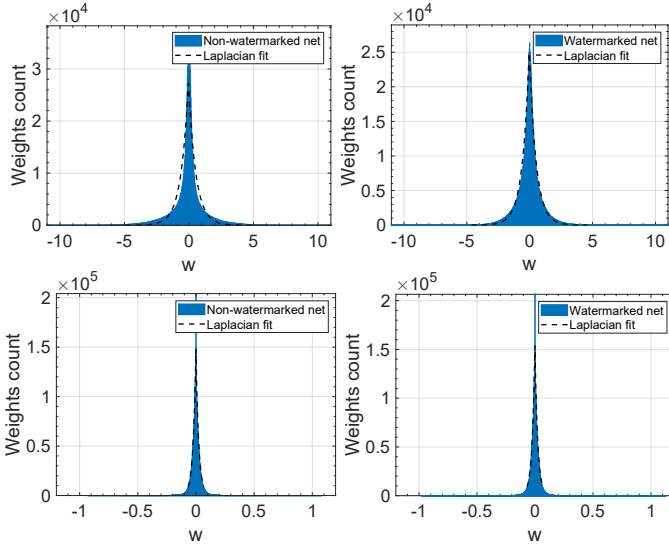


Fig. 2: Distribution of non-watermarked weights for normal (left) and watermarked (right) models, for the XceptionNet-based GAN detector (top row) and DenseNet-based GTSRB classifier (bottom row). The watermark settings in the right plots are:  $l = 256$ ,  $S = 6$ ,  $C = 1$ , single-layer, for the GAN detector and  $l = 1024$ ,  $S = 15$ ,  $C = 15$ , and 4-layers, for the GTSRB classifier.

thus confirming that the values  $C \leq 1$  are good from the point of view of the security.

For the GTSRB watermarked models, the histograms of the weights of layer 'conv4\_block20' and 'conv5\_block16' are reported in the figure, for the two settings respectively. The plots reveal that the indistinguishability is well preserved in the case considered in these plots, with  $C = 15$ . Since the variance of the weights for the layers is extremely small ( $\sigma_k = 0.00069$  for 'conv4\_block20' and  $0.00062$  for 'conv5\_block16') and the percentage of watermarked weights is much smaller than that of non-watermarked weights ( $p_k^m = 3.5\%$  for 'conv4\_block20' and  $p_k^m = 27.2\%$  for 'conv5\_block16'), the invisibility of the watermark is well preserved also with values of  $C$  larger than 1. From our experiments, we argued that values  $C$  lower than 20 are all fine. The values of KL distance between the distribution of the watermarked and non-watermarked weights (normalized histograms) for the 3 settings and embedded layers in Figure 3 are 0.154, 1.038, and 0.801 respectively. By considering the global distribution of the watermarked and non-watermarked weights over all the layers of the networks, the corresponding KL distances are 0.043, 0.217 and 0.246.

### B. Robustness evaluation

The robustness performance of the proposed watermarking method are assessed against several types of typical modifications typically undergone by neural networks: parameters pruning and weights quantization (compression), transfer learning and fine tuning (retraining). The analysis of the robustness against retraining for transfer learning is the most interesting one, being this a requirement hardly achieved by prior art methods, hence most of the results we are reporting refers to this case.

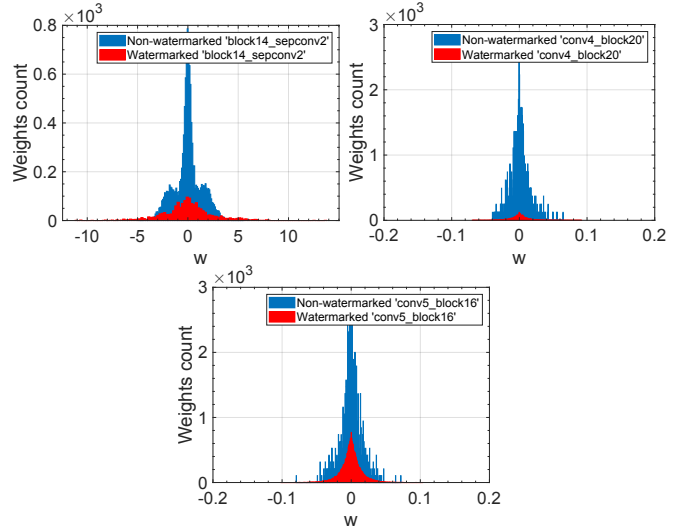


Fig. 3: Distribution of the weights in the embedding layer. From top left to bottom right: XceptionNet-based GAN detection watermarked model with  $l = 256$ ,  $S = 6$ ,  $C = 1$ , single-layer (block14\_sepconv2); DenseNet-based GTSRB classification watermarked model with  $l = 1024$ ,  $S = 15$ ,  $C = 15$ , and 4-layers (conv4\_block20 is visualized); DenseNet-based GTSRB classification watermarked model with  $l = 2048$ ,  $S = 25$ ,  $C = 15$ , 2-layers (conv5\_block16 is visualized).

As shown below, the results we got show that, when  $\gamma$  (hence  $C$ ) is not too small and the spreading factor is large enough, the watermark is extremely robust against all kinds of network modification and re-use.

1) *Model compression*: Parameter pruning is applied by cropping a fraction  $p$  of the weights in the convolutional layers by setting them to zero. As customary done, the weights are cut off based on their absolute values, from the smallest to the largest. Watermark extraction is carried out as usual. The performance are assessed for several pruning fractions  $p$ . Fig. 4 reports the results for the case of XceptionNet-based GAN detection (top) and DenseNet-based GTSRB and CIFAR-10 classification (bottom) in terms of influence in the TER and BER. The parameter setting considered for the GAN watermarked network is  $l = 256$ ,  $S = 6$ ,  $C = 1$ , while the GTSRB classifier is watermarked with  $l = 1024$ ,  $S = 20$ ,  $C = 15$  4-layers (Set# 1) and the CIFAR-10 classifier with  $l = 1024$ ,  $S = 25$ ,  $C = 20$ , 2-layers. A very similar behaviour can be observed with the other watermarking settings. The fraction of pruned weights  $p$  is provided in the x-axis. We see that, in all the cases, pruning has almost no impact on the TER when  $p$  is lower than 0.4. The BER remains zero until  $p = 0.6$  and start increasing when the network is no longer unusable ( $TER \geq 50\%$ ), thus confirming the good robustness of the watermarking scheme against model pruning.

Robustness against weights quantization is also achieved by the proposed watermarking scheme. In particular, we verified that conversion to int32, int16, int8 and int4 does not affect the BER, in all the settings considered for the various tasks, while the TER decreases to a value below or around 50% (depending on the task) with int8, that is when  $n_b = 8$  bits are considered

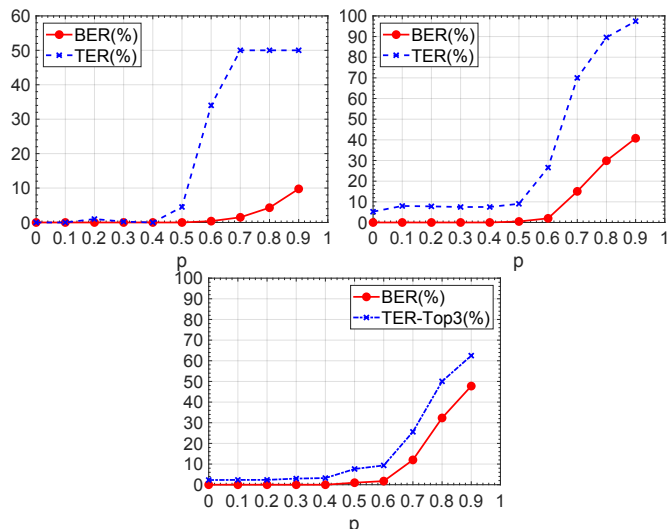


Fig. 4: Robustness performance against parameter pruning. From top left to bottom right; the watermarked GAN detector with  $l = 256$ ,  $S = 6$ ,  $C = 1$ ; the watermarked GTSRB classifier with  $l = 1024$ ,  $S = 20$ ,  $C = 15$ , 4-layers embedding; the watermarked CIFAR-10 classifier with  $l = 1024$ ,  $S = 25$ ,  $C = 20$ , 2-layers embedding.

TABLE IV: Robustness against transfer learning from GAN detection to cat&horse classification.

$l$	$S$	$C$	Layers	TER(%)	BER(%)
256	6	0.7	1	4.2	0.0
	6	1	1	5.4	0.0
1024	6	1	1	5.0	0.19
	6	1	2	4.8	0.68
	10	1	4	5.4	0

for the quantization. The robustness against quantization is not surprising and is a consequence of the fact that the sign of the weights is preserved by the quantization operation, hence the extraction of the watermark is not affected by the quantization operation.

2) *Retraining*: Table IV shows the results of the experiments regarding retraining XceptionNet from GAN face detection to cat&horse LSUN classification. The results are reported for various payloads, strengths and spreading factors. We observe that when  $l = 256$  the BER after retraining is always 0, hence robustness is achieved in all the cases. When  $l = 1024$ , the BER is close to 0 when  $S = 6$  (both for single and 2-layer embedding), and reaches 0 when  $S = 10$ . The results of transfer learning in the second scenario, where the GTSRB classification model based on DenseNet is retrained on CIFAR10, are shown in Table V. The Top-1 and Top-3 TER values are reported, where TER-Top1 is the conventional TER, while TER-Top3 refers to the TER when we measure the probability that the correct class is included among the 3 classes with the highest predicted values. As we said, these performance are aligned with those achieved by the normal model trained on the CIFAR10 task (in which case, TER-Top-1 = 19.67% and TER-Top3 = 5.62% - without augmentation. By using augmentation, that is not considered in the training of our watermarked models, the TER-Top3 for CIFAR can be

TABLE V: Robustness against transfer learning from GTSRB to CIFAR10 classification. The TER(%) and BER(%) after the retraining are reported.

$l$	$S$	$C$	Layers	TER(%) - Top1	TER(%) - Top3	BER(%)
256	6	2	1	22.68	5.54	32.42
	6	10	1	23.09	5.70	7.03
	6	15	1	22.58	5.15	1.17
	12	2	2	20.21	5.54	28.9
	12	10	2	19.41	5.70	2.35
	12	15	2	19.31	5.18	0.00
1024	20	15	2	23.77	5.55	0.00
	10	15	4 (1)	22.69	5.24	1.27
	15	15	4 (1)	21.13	4.68	0.39
	20	15	4 (1)	22.16	4.74	0.29
	25	15	4 (1)	21.20	4.34	0.00
	15	15	4(2)	21.09	4.42	0.01
	20	15	4(2)	22.93	5.43	0.00
	20	15	2	22.78	5.34	0.01
2048	25	15	2	21.65	4.68	0.00
	25	15	4(2)	22.57	5.36	0.00

TABLE VI: Robustness against fine-tuning (on 70% of the dataset) for GTSRB classification.

$l$	$S$	$C$	Layers	TER (%)	BER(%)
256	6	2	1	4.49	26.56
	6	15	1	5.19	4.32
	12	15	2	3.86	2.10
	20	15	2	5.49	0.39
1024	20	15	2	7.27	2.34
	10	15	4(1)	4.06	0.87
2048	20	15	2	4.66	1.02
	25	15	2 o 4(2)	6.93	0.78

reduced to 2.62%). We observe that, while in the XceptionNet case, watermark robustness (BER=0 after retraining) can be achieved with  $S = 6$ , with DenseNet we need to consider larger spreading factors to achieve a BER equal to 0 after the retraining. The possible reason is that in DenseNet models the absolute values taken by the weights are typically much lower than in XceptionNet models, then they are more affected by the retraining process, with the weights often changing their signs as a consequence of the retraining. This makes the use of a larger spreading factor fundamental to improve the robustness of the watermark. From the table, we see that when  $C = 15$  robustness can be achieved with  $S = 12$  for low payloads ( $l = 256$ ), while for the largest payload considered in our tests (2048 bit), we need to consider  $S = 25$ .

It is also interesting to observe how the choice of the host layers affect the results. In particular, by looking at the results for the 4 layers embedding case, a lower spreading factor is necessary with Set#2 with respect to Set#1 to get a BER equal to 0 (that is,  $S = 20$  instead of 25 for  $l=1024$ ). Moreover, for the same payload (1024 bit), a BER equal to 0 is also achieved with the 2-layers embedding for the same  $S = 20$ . More in general, we observe that, as long as the percentage of embedded weights in each layer is not too large, thus preventing the correct functionality of the network, there is no advantage in embedding the watermark in more layers with a lower percentage of host weights each, with respect to embedding the watermark in few layers with a larger percentage.

The results we got for fine-tuning are discussed below. For

the GAN detection network, we get  $BER = 0$  for all the watermark settings (in terms of payload,  $S$ , and  $C$  values) reported in Table IV. A selection of the results we got for GTSRB classification is reported in Table VI. Similar considerations to the transfer learning case can be drawn, with the BER decreasing while increasing  $S$  and  $C$ , and the choice of the host layers also affecting the results. In this case, the BER we obtain is larger than in the case of retraining for transfer learning on CIFAR-10. However, a low, although not 0, BER can be obtained for the settings with the largest  $S$  and  $C$  (we observe that the GTSRB is a small datasets, and it might also be the case that, by using 70% of the data, some classes are not very well represented).

A similar behavior was observed when the watermark is embedded in the network for CIFAR-10 classification. Some selected results are provided in Table VII and discussed in the following section. Similar considerations can be done pertaining the impact of the watermark parameters to the unobtrusiveness and the robustness, with the difference that, in the CIFAR-10 case, achieving robustness against fine-tuning requires a less demanding setting for  $S$  and  $C$  (i.e., a bit lower values) with respect to transfer-learning.

#### *Comparison with the state-of-the-art.*

In this section, we compare our method with the white-box multi-bit DNN watermarking methods of Uchida et al. [8] and Li et al. [9]. The methods have been implemented by using the code released by the authors. The DenseNet-40 architecture is considered for training. The networks are trained following the same setting in [9], embedding the watermark in the first convolutional layer of the second dense block. Table VII reports the results of these methods, compared to our method, for watermarked networks trained for CIFAR-10 and GTSRB classification, both in terms of TER, BER and robustness against fine-tuning and transfer-learning. As with our method, fine-tuning is performed by training the network for additional 10 epochs on 70% of the same dataset. Transfer learning is carried out from CIFAR-10 to GTSRB in one case and GTSRB to CIFAR-10 in the other case. For CIFAR-10, the TER(%) - Top3 is reported. We observe that, while the unobtrusiveness is good for both Uchida et al. and Li et al.'s methods, the BER is better for the Li's method, especially for large payloads, in which case the method in [9] gets BER above 10%, which is in line with the claims in the paper. However, both methods are not robust against fine tuning. Some robustness can be achieved only by Uchida's method for very low payload, i.e.,  $l = 128$ , in which case  $BER = 9.37\%$  for GTSRB and  $6.25\%$  for CIFAR-10. Robustness is even worse in the transfer learning scenario. With regard to our method, performance are reported for the 2 layers embedding case both for GTSRB and CIFAR-10. For the CIFAR-10 task, we also report the results obtained with the setting  $S = 25$  and  $C = 20$ , that was not considered in the previous experiments. In fact, we observed that, when the model is trained on the CIFAR-10 task, a larger spreading factor and/or watermark strength is necessary to get  $BER = 0\%$  after re-training (we conjecture that this is related to the fact that the magnitude of the weights for the CIFAR-10 model is very small, smaller than in the in the GTSRB case,

the variance being about a factor 2.5 less in all the layers). In the setting  $S = 25$  and  $C = 20$  for CIFAR-10, we get  $BER = 0\%$  after both fine tuning and transfer learning also when  $l = 2048$  (not reported in the table).

## VII. CONCLUDING REMARKS

We proposed a white-box DNN watermarking algorithm for multi-bit embedding that exploits a new information coding strategy to improve the robustness against network modifications and re-use. The watermark message is spread across a number of fixed weights, whose position depends on a secret key, that are set prior to training and left unchanged during the training procedure. The distribution of the watermarked weights is theoretically optimized in such a way to minimize the distinguishability between watermarked and non-watermarked weights. The experimental results show that the proposed algorithm can achieve large payloads while being robust against network modifications and re-use. In particular, robustness can be achieved in the very challenging transfer learning scenario, that is, when the protected model is used as pre-trained model for re-training the network on a different dataset and task.

As a direction for further research, we plan to carry out experiments to understand the limits of the system in terms of capacity (payload), that is, to characterize the payload that can be achieved without a significant impact on the TER. Future works will focus on a comprehensive analysis of the security of the proposed watermarking scheme against informed attackers, that is, attackers aware of the presence of the watermark, who try to erase the watermark information by embedding a new one (overwriting attacks) or try to unveil watermark parameters, e.g., by analyzing the sensitivity or impact of the weights on the classification output of the network. A very interesting direction to eventually improve the robustness of the proposed DNN watermarking system against informed attackers would be to apply channel-coding to the informative message before transforming it in the watermark signal (as done in media watermarking [39]). Investigating the kind of codes that are most suitable in the DNN watermarking scenario would also be a very relevant research.

## REFERENCES

- [1] Y. Adi, C. Baum, M. Cissé, B. Pinkas, and J. Keshet, "Turning your weakness into a strength: Watermarking deep neural networks by backdooring," in *27th USENIX Security Symposium, USENIX Security 2018, Baltimore, MD, USA, August 15-17, 2018*, W. Enck and A. P. Felt, Eds. USENIX Association, 2018, pp. 1615–1631. [Online]. Available: <https://www.usenix.org/conference/usenixsecurity18/presentation/adi>
- [2] Y. Li, H. Wang, and M. Barni, "A survey of deep neural network watermarking techniques," *Neurocomputing*, vol. 461, pp. 171–193, 2021. [Online]. Available: <https://www.sciencedirect.com/science/article/pii/S092523122101095X>
- [3] C. I. Podilchuk and E. J. Delp, "Digital watermarking: algorithms and applications," *IEEE Signal Processing Magazine*, vol. 18(4), no. 4, pp. 33–46, 2001.
- [4] I. J. Cox, M. L. Miller, J. A. Bloom, and C. Honsinger, *Digital Watermarking*. Springer, 2002, vol. 53.
- [5] M. Barni and F. Bartolini, *Watermarking systems engineering: enabling digital assets security and other applications*. Crc Press, 2004.
- [6] M. Barni, F. Pérez-González, and B. Tondi, "Dnn watermarking: Four challenges and a funeral," in *Proceedings of the 2021 ACM Workshop on Information Hiding and Multimedia Security*, 2021, pp. 189–196.

TABLE VII: Comparison with existing methods. TER and BER are reported in % (FT = fine tuning, TL = transfer learning). The baseline accuracy is 6.12% for GTSRB and 5.62% (Top-3) for CIFAR-10.

Task	Payload	Uchida et al. [8]						Li et al. [9]						Proposed										
		TER		BER		After FT		After TL		TER		BER		After FT		After TL		(S,C)	TER	BER	After FT		After TL	
		TER	BER	TER	BER	TER	BER	TER	BER	TER	BER	TER	BER	TER	BER	TER	BER				TER	BER		
GTSRB	128	5.97	3.12	1.66	<b>9.37</b>	4.97	<b>17.18</b>	4.44	0	4.33	<b>50.00</b>	3.64	<b>48.43</b>	(12,15)	9.40	0	6.39	<b>0</b>	5.81	<b>0</b>				
	256	5.54	6.64	6.47	<b>24.21</b>	4.58	<b>45.31</b>	3.89	0	2.06	<b>46.48</b>	9.17	<b>49.60</b>	(20,15)	6.89	0	5.49	<b>0.39</b>	6.31	<b>0</b>				
	1024	2.85	14.16	5.06	<b>27.14</b>	3.54	<b>29.39</b>	4.15	4.39	5.79	<b>48.92</b>	4.63	<b>49.90</b>	(20,15)	5.79	0	7.27	<b>2.34</b>	5.55	<b>0</b>				
CIFAR-10	128	3.73	1.56	2.55	<b>6.25</b>	5.06	<b>17.18</b>	3.70	0	5.84	<b>53.12</b>	8.42	<b>42.96</b>	(12,15)	2.39	0	2.11	<b>0.78</b>	10.50	<b>16.48</b>				
	256	5.23	4.68	4.61	<b>19.14</b>	4.34	<b>23.43</b>	4.12	0	2.87	<b>51.95</b>	4.30	<b>50.00</b>	(12,15)	2.46	0	2.05	<b>2.73</b>	7.59	<b>12.89</b>				
	1024	4.08	13.37	5.17	<b>26.85</b>	2.59	<b>32.32</b>	2.69	1.46	4.07	<b>51.36</b>	7.89	<b>51.17</b>	(20,15)	2.42	0	2.01	<b>0.29</b>	7.27	<b>2.34</b>				
														(25,20)	2.28	0	2.60	<b>0</b>	9.32	<b>0</b>				

- [7] S. J. Pan and Q. Yang, "A survey on transfer learning," *IEEE Transactions on knowledge and data engineering*, vol. 22, no. 10, pp. 1345–1359, 2009.
- [8] Y. Uchida, Y. Nagai, S. Sakazawa, and S. Satoh, "Embedding watermarks into deep neural networks," in *Proceedings of the 2017 ACM on International Conference on Multimedia Retrieval*, 2017, pp. 269–277.
- [9] Y. Li, B. Tondi, and M. Barni, "Spread-transform dither modulation watermarking of deep neural network," in *EURASIP Journal on Information Security*.
- [10] M. Kuribayashi, T. Tanaka, and N. Funabiki, "Deepwatermark: Embedding watermark into dnn model," in *2020 Asia-Pacific Signal and Information Processing Association Annual Summit and Conference (APSIPA ASC)*. IEEE, 2020, pp. 1340–1346.
- [11] J. Wang, H. Wu, X. Zhang, and Y. Yao, "Watermarking in deep neural networks via error back-propagation," *Electronic Imaging*, vol. 2020, no. 4, pp. 22–1, 2020.
- [12] T. Wang and F. Kerschbaum, "Robust and undetectable white-box watermarks for deep neural networks," *arXiv preprint arXiv:1910.14268*, 2019.
- [13] —, "Attacks on digital watermarks for deep neural networks," in *ICASSP 2019-2019 IEEE International Conference on Acoustics, Speech and Signal Processing (ICASSP)*. IEEE, 2019, pp. 2622–2626.
- [14] M. Shafiqnejad, N. Lukas, J. Wang, X. Li, and F. Kerschbaum, "On the robustness of backdoor-based watermarking in deep neural networks," in *Proceedings of the 2021 ACM Workshop on Information Hiding and Multimedia Security*, 2021, pp. 177–188.
- [15] E. Tartaglione, M. Grangetto, D. Cavagnino, and M. Botta, "Delving in the loss landscape to embed robust watermarks into neural networks," in *2020 25th International Conference on Pattern Recognition (ICPR)*. IEEE, 2021, pp. 1243–1250.
- [16] A. P. Maung Maung and H. Kiya, "Piracy-resistant dnn watermarking by block-wise image transformation with secret key," in *Proceedings of the 2021 ACM Workshop on Information Hiding and Multimedia Security*, ser. IH&MMSec '21. New York, NY, USA: Association for Computing Machinery, 2021, p. 159–164. [Online]. Available: <https://doi.org/10.1145/3437880.3460398>
- [17] C.-S. Lu, "Sparse trigger pattern guided deep learning model watermarking," in *Proceedings of the 2022 ACM Workshop on Information Hiding and Multimedia Security*, ser. IH&MMSec '22. New York, NY, USA: Association for Computing Machinery, 2022, p. 33–38. [Online]. Available: <https://doi.org/10.1145/3531536.3532961>
- [18] H. Chen, B. D. Rouhani, C. Fu, J. Zhao, and F. Koushanfar, "Deepmarks: A secure fingerprinting framework for digital rights management of deep learning models," in *Proceedings of the 2019 on International Conference on Multimedia Retrieval*, 2019, pp. 105–113.
- [19] T. Wang and F. Kerschbaum, "Riga: Covert and robust white-box watermarking of deep neural networks," in *Proceedings of the Web Conference 2021*, 2021, pp. 993–1004.
- [20] T. Yasui, T. Tanaka, A. Malik, and M. Kuribayashi, "Coded dnn watermark: Robustness against pruning models using constant weight code," *Journal of Imaging*, vol. 8, no. 6, p. 152, 2022.
- [21] J. Zhang, Z. Gu, J. Jang, H. Wu, M. P. Stoeklin, H. Huang, and I. Molloy, "Protecting intellectual property of deep neural networks with watermarking," in *Proceedings of the 2018 on Asia Conference on Computer and Communications Security*, 2018, pp. 159–172.
- [22] B. Darvish Rouhani, H. Chen, and F. Koushanfar, "Deepsigns: An end-to-end watermarking framework for ownership protection of deep neural networks," in *Proceedings of the Twenty-Fourth International Conference on Architectural Support for Programming Languages and Operating Systems*, 2019, pp. 485–497.
- [23] L. Fan, K. W. Ng, and C. S. Chan, "Rethinking deep neural network ownership verification: Embedding passports to defeat ambiguity attacks," in *Advances in Neural Information Processing Systems*, H. Wallach, H. Larochelle, A. Beygelzimer, F. Alché-Buc, E. Fox, and R. Garnett, Eds., vol. 32. Curran Associates, Inc., 2019. [Online]. Available: <https://proceedings.neurips.cc/paper/2019/file/75455e062929d32a333868084286bb68-Paper.pdf>
- [24] B. W. Guo and M. Barni, "Masterface watermarking for ipr protection of siamese network for face verification," in *International Workshop on Digital-forensics and Watermarking*, November 2021.
- [25] B. D. Rouhani, H. Chen, and F. Koushanfar, "Deepsigns: an end-to-end watermarking framework for protecting the ownership of deep neural networks," in *ACM International Conference on Architectural Support for Programming Languages and Operating Systems*, 2019.
- [26] Y. Li, L. Abady, H. Wang, and M. Barni, "A feature-map-based large-payload dnn watermarking algorithm," in *International Workshop on Digital Watermarking*. Springer, 2021, pp. 135–148.
- [27] B. Cortiñas-Lorenzo and F. Pérez-González, "Adam and the ants: On the influence of the optimization algorithm on the detectability of dnn watermarks," *Entropy*, vol. 22, no. 12, 2020. [Online]. Available: <https://www.mdpi.com/1099-4300/22/12/1379>
- [28] T. M. Cover and J. A. Thomas, *Elements of Information Theory*. New York: Wiley Interscience, 1991.
- [29] M. L. Miller, G. J. Doërr, and I. J. Cox, "Applying informed coding and embedding to design a robust high-capacity watermark," *IEEE Transactions on image processing*, vol. 13, no. 6, pp. 792–807, 2004.
- [30] I. Goodfellow, J. Pouget-Abadie, M. Mirza, B. Xu, D. Warde-Farley, S. Ozair, A. Courville, and Y. Bengio, "Generative adversarial networks," *Communications of the ACM*, vol. 63, no. 11, pp. 139–144, 2020.
- [31] S. Houben, J. Stallkamp, J. Salmen, M. Schlipsing, and C. Igel, "Detection of traffic signs in real-world images: The German Traffic Sign Detection Benchmark," in *International Joint Conference on Neural Networks*, no. 1288, 2013.
- [32] A. Krizhevsky, G. Hinton *et al.*, "Learning multiple layers of features from tiny images," 2009.
- [33] T. Karras, S. Laine, M. Aittala, J. Hellsten, J. Lehtinen, and T. Aila, "Analyzing and improving the image quality of StyleGAN," in *Proc. CVPR*, 2020.
- [34] D. Gragnaniello, D. Cozzolino, F. Marra, G. Poggi, and L. Verdoliva, "Are gan generated images easy to detect? a critical analysis of the state-of-the-art," in *2021 IEEE International Conference on Multimedia and Expo (ICME)*. IEEE, 2021, pp. 1–6.
- [35] [Online]. Available: <https://github.com/andreacos/gan-generated-face-detection>
- [36] G. Huang, Z. Liu, L. Van Der Maaten, and K. Q. Weinberger, "Densely connected convolutional networks," in *Proceedings of the IEEE conference on computer vision and pattern recognition*, 2017, pp. 4700–4708.
- [37] [Online]. Available: <https://github.com/titu1994/DenseNet>
- [38] F. Yu, Y. Zhang, S. Song, A. Seff, and J. Xiao, "Lsun: Construction of a large-scale image dataset using deep learning with humans in the loop." *CoRR*, vol. abs/1506.03365, 2015. [Online]. Available: <http://dblp.uni-trier.de/db/journals/corr/corr1506.html#YuZSSX15>
- [39] F. Pérez-González, J. R. Hernández, and F. Balado, "Approaching the capacity limit in image watermarking: a perspective on coding techniques for data hiding applications," *Signal Processing*, vol. 81, no. 6, pp. 1215–1238, 2001.